Laminin Forms an Independent Network in Basement Membranes

Peter D. Yurchenco, Yi-Shan Cheng, and Holly Colognato

Department of Pathology, Robert Wood Johnson Medical School, Piscataway, New Jersey 08854

Abstract. Laminin self-assembles in vitro into a polymer by a reversible, entropy-driven and calcium-facilitated process dependent upon the participation of the short arm globular domains. We now find that this polymer is required for the structural integrity of the collagen-free basement membrane of cultured embryonal carcinoma cells (ECC) and for the supramolecular organization and anchorage of laminin in the collagen-rich basement membrane of the Engelbreth-Holm-Swarm tumor (EHS). First, low temperature and EDTA induced the dissolution of ECC basement membranes and released ~80% of total laminin from the EHS basement membrane. Second, laminin elastase fragments (E4 and E1′) possessing the short arm globules of the B1, B2, and A chains selectively acted as competitive ligands that dissolved ECC basement membranes and displaced laminin from the EHS basement membrane into solution. The fraction of laminin released increased as a function of ligand concentration, approaching the level of the EDTA-reversible pool. The smaller (~20%) residual pool of EHS laminin, in contrast, could only be effectively displaced by E1′ and E4 if the collagenous network was first degraded with bacterial collagenase. The supramolecular architecture of freeze-etched and platinum/carbon replicated reconstituted laminin gel polymer, ECC, and collagenase-treated EHS basement membranes were compared and found to be similar, further supporting the biochemical data. We conclude that laminin forms a network independent of that of type IV collagen in basement membranes. Furthermore, in the EHS basement membrane four-fifths of laminin is anchored strictly through noncovalent bonds between laminin monomers while one-fifth is anchored through a combination of these bonds and laminin-collagen bridges.

LAMININ and its genetic isoforms are major constituents of basement membranes. As isolated from the Engelbreth-Holm-Swarm (EHS)[1] tumor, laminin is a large four-armed glycoprotein (≥800 kD), formed from three polypeptide chains (A, B1, B2): each of the shorter arms possesses amino-terminal and more included globular domains separated by segments composed of EGF-like repeats (Beck et al., 1990). Purified laminin can polymerize in the presence of Ca^{2+} in a concentration- and temperature-dependent manner and there is both electron microscopic and biochemical evidence that the short arm globular domains are required for this assembly (Yurchenco et al., 1985; Schittny and Yurchenco, 1990). Laminin is the only basement membrane component other than type IV collagen (Yurchenco and Schittny, 1990) known to polymerize and therefore is likely to be the only major polymer in some newly formed basement membranes which initially lack type IV collagen (Form et al., 1986; Timpl, 1989).

Evidence that this polymerization process occurs in vivo, that a similar molecular architecture is formed by cells, and that this architecture contributes an important part of basement membrane architecture has been lacking until now. To directly address the assembly and architecture of laminin in the extracellular matrices produced by cells, we have used a combination of competitive ligand extraction and high resolution metal replication to analyze laminin in the basement membrane of embryonal carcinoma cells (ECC) as well as the more complex type IV collagen-rich basement membrane of the EHS tumor. The ECC, grown in tissue culture, can form enlarging blastula-like cell spherules that consist of an outer cell layer and an inner extracellular matrix core rich in laminin but devoid of type IV collagen (Brauer and Keller, 1989). The EHS tumor basement membrane, which represents half of total tumor mass, contains laminin, entactin (nidogen), type IV collagen, and smaller amounts of other components such as the heparan sulfate proteoglycan and BM-40 (Timpl, 1989).

In this study we present both biochemical and morphological evidence that laminin polymers form an essential part of basement membrane molecular architecture and that the short arm domains of laminin are required for laminin's structural integrity in basement membranes. Furthermore, these studies reveal that there is heterogeneity of laminin structure in the EHS tumor basement membrane in which a fraction of the laminin is anchored to type IV collagen while nearly all laminin is immobilized through self-interactions.

1. *Abbreviations used in this paper*: ECC, embryonal carcinoma cells; EHS, Engelbreth-Holm-Swarm tumor.

Materials and Methods

Preparation and Labeling of Laminin and Its Fragments

Purification steps were carried out at 0–5°C. Laminin was isolated from lathyritic EHS tumor based on the EDTA-extraction method of Paulsson et al. (1987*a*) and purified by Sephacryl HR400 (Pharmacia Fine Chemicals, Piscataway, NJ) gel filtration and DEAE-Sephacel ion exchange chromatography without the use of chaotropic agents as described (Schittny and Yurchenco, 1990). The unbound peak from the DEAE column consisted of laminin while the first bound peak consisted of the laminin–entactin (laminin–nidogen) complex. The unbound laminin was used for the polymerization assay described below. The elastase fragments E1′ and E4 of laminin were generated at an enzyme-substrate ratio of 1:200 to 1:400 (optimal ratio determined experimentally for each lot of enzyme) at 25°C for 23 h and purified by Sepharose CL-6B gel filtration (Pharmacia Fine Chemicals) and HPLC DEAE-5PW ion exchange (TosoHAAS, Philadelphia, PA) as previously described (Schittny and Yurchenco, 1990). Laminin was stored in 50 mM Tris-HCl, pH 7.4, containing 90 mM NaCl (TBS) and 0.1 mM EDTA. Fragment P1′ was purified from a pepsin digest of laminin by Agarose 1.5-m gel filtration (Calbiochem Corp., La Jolla, CA) in 1 M calcium chloride as described (Schittny and Yurchenco, 1990). Laminin was radioiodinated with ^{125}I-Na by a lactoperoxidase method and purified by chromatography on a Sepharose CL-6B column (Schittny and Yurchenco, 1990). Type IV collagen was extracted with 2 M guanidine-HCl (GuHCl)/10 mM dithiothreitol and purified by several cycles of precipitation with 1.7 M NaCl and DEAE-cellulose ion exchange as previously described (Yurchenco and Furthmayr, 1984). Collagen chains lacking the COOH-terminal globule, but otherwise intact, were prepared by limited pepsin digestion and gel filtration on Sephacryl S1000 (Pharmacia Fine Chemicals) as described in detail by Yurchenco and Furthmayr (1984).

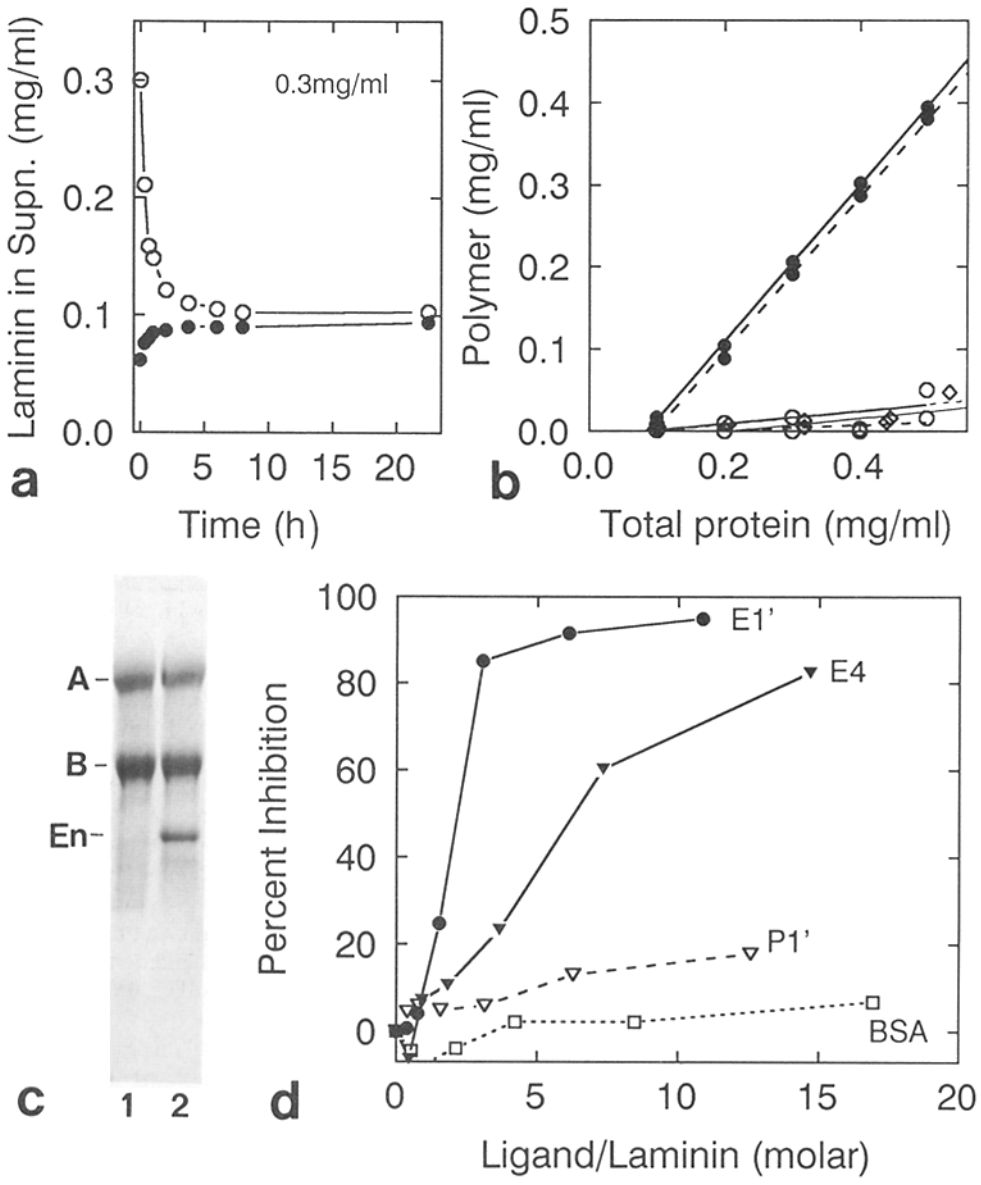

Figure 1. Self-assembly of laminin in vitro. (*a*) Reversibility of polymerization. Laminin (1 mg/ml), maintained on ice, was divided into two groups (each 5 ml). The first was incubated (polymerized) at 37°C for 1 h followed by dilution to 0.3 mg/ml (at 0 h) to allow subsequent dissociation (●). The second was diluted to 0.3 mg/ml followed by incubation at 37°C (at 0 h) to induce polymerization (○). At the indicated times, 0.5-ml aliquots were centrifuged and the concentration of laminin was determined in the supernatant (free laminin concentration). Regardless of initial polymer state, the concentration of free laminin converged to the value (0.1 mg/ml) of the free critical concentration. (*b*) Concentration dependency of polymerization for laminin (---) and the laminin/entactin complex (——). Incubation (in TBS) was carried out either at 37°C in the presence of 1 mM $CaCl_2$ (●) 5 mM EDTA (○) or on ice (0°C) in 1 mM $CaCl_2$ (◇). A critical concentration of 0.1 mg/ml was determined for laminin and laminin/entactin with no significant difference noted in behavior between the two components. Formation of sedimentable aggregates required the presence of calcium and heat. (*C*) SDS–polyacrylamide gel of laminin (lane *1*) and laminin/entactin (lane *2*). The samples were electrophoresed on a 3.5–12% gradient gel under reducing conditions and were stained with Coomassie blue (*A*, A chain; *B*, B chain; *En*, entactin). (*d*) Competitive inhibition of polymerization using the protein ligands E1′ (elastase-generated short arm complex of laminin/entactin), E4 (elastase fragment consisting of B1 chain outer globule and EGF stem), P1′ (pepsin-generated short arm complex of laminin lacking globular domains), and BSA. These ligands were incubated with ^{125}I-laminin (0.25 mg/ml) in 0.1-ml aliquots at 37°C. Only fragments possessing short arm globular domains were observed to significantly inhibit laminin polymerization.

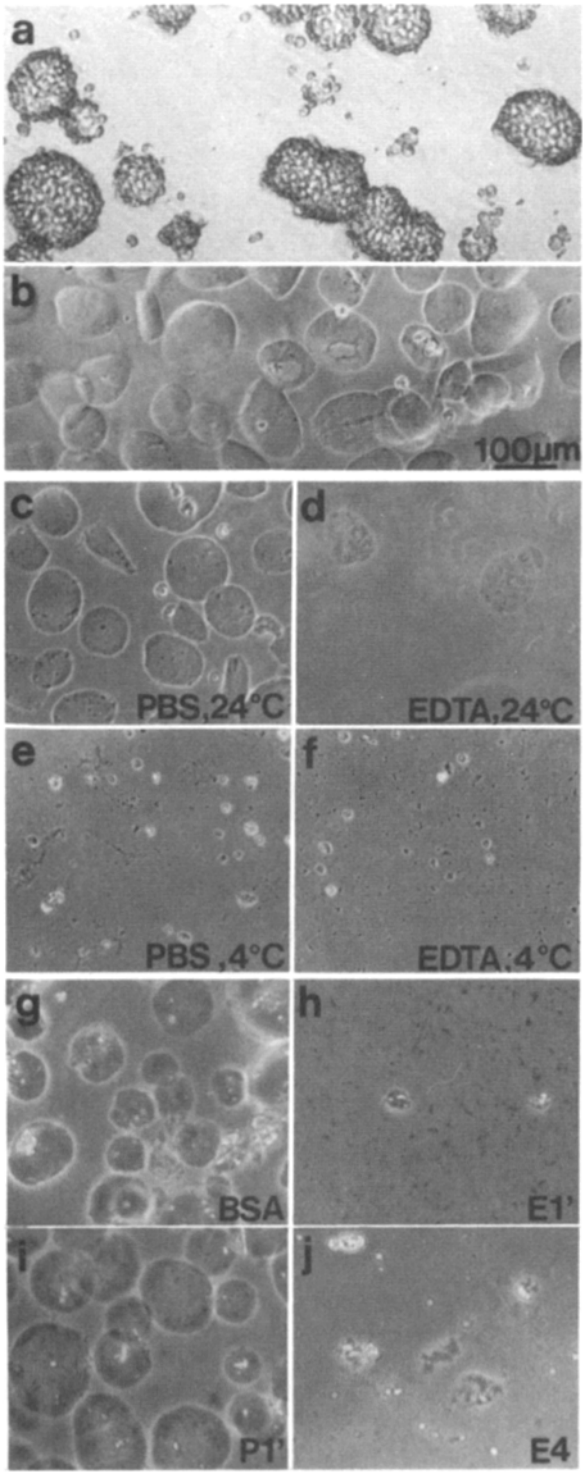

Figure 2. Effect of temperature, EDTA, and ligands on integrity of embryonal carcinoma basement membranes (phase micrographs). (*a*) M1536-B3 ECC spherules after growth in culture medium. (*b*) Basement membranes (cores) isolated from spherules with cytochalasin B as described. (*c–j*) Isolated basement membranes maintained for 1 d in PBS at room temperature (*c*), 10 mM EDTA in PBS under same conditions (*d*), PBS at 4°C (*e*), 10 mM EDTA at 4°C (*f*), and in PBS in the following ligands (10 μM) at 37°C for 1 d: BSA (*g*), E1′ (*h*), P1′ (*i*), and E4 (*j*). The same conditions (low temperature, EDTA, E1′, and E4) which inhibited laminin polymerization caused the dissolution of the basement membranes.

Determination of Protein Concentration, SDS-PAGE and Fluorography

Protein in solution was determined either by absorbance at 280 nm (for protein cleared of turbid material), colorimetrically (Schittny and Yurchenco, 1990), or for pepsin-treated type IV collagen (465 kD), by dry weight (Yurchenco and Furthmayr, 1984). The absorbance (280 nm) extinction coefficients used were $\epsilon = 750$ gm^{-1}cm^2 for laminin (710 kD) and laminin/entactin (835 kD) (Yurchenco et al., 1990), $\epsilon = 889$ gm^{-1}cm^2 for E1′ (450 kD) (Paulsson, 1988) and P1′ (350 kD), and $\epsilon = 670$ gm^{-1}cm^2 for BSA.

SDS-PAGE was carried out in 5% or 3.5–12% linear gradient gels (Laemmli, 1970) as described in Yurchenco et al. 1990) and stained with Coomassie brilliant blue R250. Molecular weight standards used were β-galactosidase (116 kD), phosphorylase B (97.4 kD), BSA (66.2 kD), and ovalbumin (42.7 kD). For fluorography, the gels, with or without previous staining, were soaked in EN^{3}HANCE (New England Nuclear, Boston, MA), transferred to water to precipitate the fluors, sandwiched between filter paper and plastic wrap, and then dried under vacuum. The dried gels were placed into x-ray cassettes with preflashed film (X-omat; Eastman Kodak Co., Rochester, N.Y.), stored at −110°C for several days, warmed to room temperature, and developed with GBX solution (Eastman Kodak Co.).

Sedimentation Assays for Laminin Polymerization

Direct Assay. Laminin samples (0.5 ml) were incubated in TBS containing 1 mM $CaCl_2$ at 35°C for 60 min in 1.5-ml Eppendorf tubes and were centrifuged at 10,500 rpm (16,000 *g*) in a microcentrifuge. The laminin concentration was determined in the supernatant at the beginning of the incubation and after centrifugation by measuring the absorbance at 280 nm as previously described (Yurchenco et al., 1990). The fraction of polymer was calculated by subtracting the supernatant concentration after centrifugation from the total laminin concentration.

Inhibition Assay. Samples with constant ^{125}I-laminin (0.25 mg/ml, 35,000–50,000 cpm/mg), but variable concentrations (0–1.6 mg/ml) of unlabeled ligand (laminin fragments, or BSA) (Sigma Chemical Co., St. Louis, MO) were incubated under the above conditions. After sedimentation, the fractional inhibition was calculated from $(L\text{-}F)/(L)$ where L is the laminin radioactivity precipitated in the absence of fragment and F is the laminin radioactivity precipitated in the presence of fragment.

Cell Culturing and Isolation of ECC Tissue Culture Basement Membranes

Stock cultures of the M1536-B3 mouse ECC line (kindly provided by Dr. Albert Chung, University of Pittsburgh, Pittsburgh, PA) (Chung et al., 1977) were grown in DME (high glucose) containing 10% FCS (Upstate Biotechnology, Inc., Lake Placid, NY) in tissue culture flasks (75 cm^2) (Corning Glass Inc., Corning, NY). The cells were incubated in humidified 5% CO_2 air at 37°C. Cells were detached by trypsinization and resuspended in fresh medium every 3 d. To obtain cell spherules with inner basement membrane cores, the trypsinized cells were transferred to 150-mm bacterial culture dishes in ~20 ml medium and grown as suspension cultures. To isolate the basement membrane cores, spherules were harvested after 9–11 d, washed by centrifugation, and resuspended in 10 ml of PBS to which cytochalasin B was added (Sigma Chemical Co.) at a final concentration of 30–40 μg/ml. The suspension was maintained at 37°C for 3–6 h with frequent agitation. At the end of the incubation the suspension was agitated vigorously, and the basement membranes were purified by low speed differential centrifugation as previously described (Chung et al., 1977). These structures were stored in concentrated suspension at 19–20°C.

Analysis of ECC Basement Membrane Dissolution

The ECC basement membranes (0.5 to 2 × 10^4 cores), which typically measured from 0.05 to 0.2 mm in diameter, were placed into an optical chamber created by gluing a plastic washer (0.9 cm i.d. × 0.3 cm) onto tissue culture plates. The cores were then mixed with PBS with or without 10 mM EDTA or protein ligand (10 μM) at a final volume of 0.2 ml containing 0.01% sodium azide to inhibit microbial growth. The chamber was closed with a glass coverslip bonded to the washer with silicone grease to prevent evaporation and to create an optically flat chamber for phase microscopy. The chambers were incubated at 0–4°C, room temperature, or on a heating block maintained at 37°C. In time course experiments, the chambers were examined at each time point with an inverted phase microscope (Olympus Corp., Lake Success, NY) fitted with a 35-mm camera and four

photographs were taken (4× objective) per sample under phase from four different fields (each 2.7 × 1.8 mm). The number of surviving core structures was counted from each photograph and summed for each well (covering one third of the entire field). Several wells were set up for each ligand condition and examined and photographed at each time point to permit determination of an average and standard error.

Biosynthetic Labeling of Laminin in EHS Basement Membrane and Analysis of Laminin Solubilization

Swiss Webster mice bearing EHS tumor (lathyritic) were injected with 1 mCi/mouse with [^{35}S]methionine and cysteine (Tran^{35}S-label, a metabolic protein labeling reagent derived from an *Escherichia coli* lysate containing 70% methionine and 15% cysteine, sp act > 1,000 Ci/mmol, ICN Flow, Costa Mesa, CA). The tumors were harvested 2 d later. For competitive displacement of tumor basement membrane laminin into solution, the tumor, maintained at room temperature, was homogenized into small fragments (to increase surface area/mass ratio), and then washed at room temperature with TBS containing 1,10-phenanthroline (1 mM) to inhibit an endogenous metaloproteinase found to otherwise cause partial degradation of the A chain of laminin in long-term incubations. The washed tumor matrix was then mixed with 0–30 μM protein ligand in a final volume of 70 μl and incubated at 37°C overnight in 1.5-ml Eppendorf tubes on a shaker platform. The tubes were centrifuged at 9,000 rpm for 5 min and the supernatants were removed. An additional 50 μl TBS was added to each tube and the tube was recentrifuged. The wash was added to the extract. The tumor residue was then extracted with 10 mM EDTA in TBS at 5°C for several hours, centrifuged as above, and the residue re-extracted with EDTA with the supernatants combined. This fraction contained the remainder of the EDTA-extractable pool of laminin. The size of the EDTA and residue pools of laminin were determined as follows. Washed EHS matrix was first extracted with 10 mM EDTA and the supernatants were obtained as described above. The residual pool was mixed with SDS-solubilizing buffer (3% SDS, 2 M urea, 63 mM Tris-HCl, pH 6.9, 2 mM EDTA), boiled for 5 min, centrifuged, and the supernatant saved. This removed the remaining laminin in the tumor.

In some experiments, either the washed EHS matrix or the matrix residue was incubated with 0.2 mg/ml bacterial collagenase (CLSPA grade, lot 77593M, 678 units/mg; Worthington Biochem. Corp., Freehold, NJ) on a shaker at room temperature or 37°C overnight in TBS containing 2 mM $CaCl_2$. The specificity of the enzyme was first evaluated by a trial overnight incubation of aliquots of EHS matrix with or without enzyme. The above lot produced no detectable degradation of laminin (relative to control) and was used in the study. Some lots of collagenase were considered unsuitable for the study because they were found to partially degrade the A chain.

Quantitation of Laminin Extracted from the EHS Matrix

^{35}S-labeled Laminin. The radiolabeled A and B chain bands were cut out of dried stained polyacrylamide gels previously impregnated with EN^{3}HANCE, placed in 7-ml glass scintillation vials, mixed with 0.35 ml of BTS-450 tissue solubilizer (Beckman Instruments, Inc., Fullerton, CA) and 0.15 ml water, incubated at 50–60°C for 2–3 h, and then mixed with 5 ml Esoscint A scintillation cocktail (National Diagnostics Inc., Manville, NJ). Radioactivity was determined using a liquid scintillation system (model LS-6000; Beckman Instruments) equipped with automatic color quenching correction and chemiluminescence detector. A quench curve for ^{35}S-label with increasing concentrations of TCA was measured and stored in the instrument computer. dpm were calculated from cpm and used for the calculations of this study.

Unlabeled Laminin. The total protein concentration of EHS tumor extract was determined colorimetrically as described above. An aliquot was separated into its component proteins by SDS-PAGE and stained with Coomassie blue. The wet gel was then scanned with a gel scanner (model 300A, Molecular Dynamics, Sunnyvale, CA) and the fraction of laminin determined. The laminin concentration was calculated by multiplying this fraction by the total protein concentration.

Platinum/Carbon Replication and EM

Glycerol Rotary Shadow Pt/C Replication of Individual Molecules. Protein samples were either dialyzed into 0.15 M ammonium bicarbonate/acetate, pH 7.4, or diluted into the same buffer and adjusted to 55% glycerol. The solution was nebulized onto freshly cleaved mica, evacuated either in a BAF400T or BAF500K freeze-etch unit (EM division of Balzers, recently reorganized as Bal-Tec, Middlebury, CT) at room temperature, and then cooled below 98°K and shadowed with 0.8–0.9 nm (determined with a quartz crystal monitor) Pt/C at an 8 or 10° angle on a rotating stage (100–120 rpm). The replicas were examined in an electron microscope (model 420; Philips Electronic Instruments Co., Mahwah, NJ) at 80 kV with a 30-μm objective aperture.

Freeze Etch and Replication of Protein Polymers and Cell Culture and Tissue Basement Membrane. Laminin polymers were freeze fixed in a buffer of proper ionic strength and pH that supports polymerization in biochemical assays (formaldehyde induces depolymerization and low salt disrupts polymer structure). While freeze fixation in isotonic salt was found to be the best method of structural preservation of laminin, thin salt deposits can accrete on the surface during etching, focally obscuring molecular details or thickening network filaments. Reconstituted laminin gels were prepared by incubating laminin/entactin on gold 400 mesh grids or directly on the copper planchets at or above 3 mg/ml in TBS containing 1 mM $CaCl_2$ at 37°C for one half to several hours. EHS tumor matrix samples were prepared by incubating ground EHS tumor particles in DNase (0.15 μg/ml) (Bethesda Research Laboratories, Gaithersburg, MD) (to remove contaminating cellular DNA) overnight at room temperature in TBS containing 4 mM $MgCl_2$. The tumor matrix was frozen on gold grids sandwiched between copper planchets without further treatment, or after selective extraction of laminin with 2 M guanidine-HCl (0–5°C) in TBS or removal of collagen by digestion with bacterial collagenase (Worthington Biochemical Corp., CLSPA, 0.2 mg/ml) overnight at room temperature or 37°C followed by centrifugation/resuspension in TBS buffer. ECC basement membrane cores were sandwiched between two copper planchets (double replica specimen carriers, Bal-Tec) inserted into the holder of a propane freeze jet device (model JFD 030; Bal-Tec), and rapidly frozen with a high pressure jet of propane cooled to 88°K. This method of freezing (>20,000°C/s according to the manufacturer) yielded the least degree of identifiable freezing artifact (i.e., large holes in the network arrays) and the most reproducible network structures. The planchets, after freezing, were transferred to liquid nitrogen and inserted into a spring-loaded double replica table, placed in the vacuum lock of the BAF500K unit previously cooled to 133°K, evacuated to 1–5 × 10^{-7} mBar, transferred to the cryopumped ultra-high vacuum (UHV) chamber (2–4 × 10^{-9} mBar), and warmed to 170°K. The sample was then fractured, deep etched at 170°K for 30 min, and cooled down to 11–13°K. The stage was rotated (80–100 rpm) and the sample shadowed with 1.0–1.2 nm Pt/C at either a 45 or 60° angle followed by a carbon support backing of ~12 nm at a 90° angle. The sample was warmed, removed from the vacuum chamber, and adherent protein/tissue removed by immersing the copper grids in 70% sulfuric acid or 100% hydrofluoric acid for several days. The replicas were transferred to water and either examined on 400-mesh gold or copper grids in the electron microscope. Stereo pairs were produced by taking photographs at 10° angle intervals.

Photography. Electron micrographs were prepared contrast reversed at intermediate contrast to enhance perception of the images.

Results

Laminin Self-assembly In Vitro

Laminin polymerization was found to obey the characteristics of a classical nucleation-propagation assembly (Fig. 1). Polymerization was completely reversible with a fixed critical concentration (0.1 mg/ml) of free protomers independent of total protein concentration and initial polymeric state (Fig. 1, *a* and *b*). Regardless of whether starting from a polymeric (Fig. 1 *a*, •), or monomeric state (Fig. 1 *a*, ○), the free (supernatant) concentration of laminin converged, as a function of time, on the critical concentration. The critical concentration could also be measured by plotting the total laminin concentration against the sedimented concentration (Fig. 1 *b*). Polymerization required the presence of divalent cations (calcium) and proceeded at 37°C but not 0°C. No difference in the dependency on concentration, temperature, or calcium was observed between laminin and the laminin–entactin complex (Fig. 1, *b* and *c*). Entactin (Carlin et al.,

1981) is a sulfated glycoprotein normally strongly bound (Timpl, 1989) to the short B2 arm near the junction of domains III and IV: we concluded that it is not required for polymerization and has no effect on the overall thermodynamics of assembly.

Defined fragments of laminin have proved useful tools to study the regions of laminin involved in polymerization (Paulsson, 1988; Schittny and Yurchenco, 1990). Elastase-generated fragment E1′ (Paulsson, 1988; similar or identical to E1X-Nd described by Mann et al., 1988) possesses the stub (domain III) of the B1 chain, the short arms of the B2 and A chains with their globular domains (Paulsson, 1988; Schittny and Yurchenco, 1990] and lesser quantities (~25%) of bound fragmented entactin (Dziadek et al., 1985). Fragment E4 represents the NH_2-terminal globule (domain VI) and adjacent EGF repeat region (domain V) of the B1 chain (Fujiwara et al., 1988). Fragment P1′ is similar to E1′ except that it lacks globular domains and entactin (Schittny and Yurchenco, 1990). Laminin polymerization was substantially inhibited in a concentration-dependent manner by short arm fragments E1′ and E4, a small to negligible degree by P1′ and not at all by BSA (Fig. 1 *d*). On a molar basis, E1′ had the most potent activity. Thus, in agreement with previous studies (Schittny and Yurchenco, 1990), fragments of laminin possessing short arm globules inhibited polymerization. This property was used to characterize laminin within basement membranes formed by cells in tissue culture and in cells.

Basement Membrane Integrity of the M1536-B3 ECC

When grown in polystyrene (bacteriological grade) plastic dishes, the cells formed multicellular spherules consisting of an outer cell layer and inner basement membrane core (Fig. 2, *a* and *b*) rich in laminin and entactin but lacking type IV collagen (see Chung et al., 1977; Brauer and Keller, 1989). When the isolated basement membrane cores were incubated overnight at 0–4°C in PBS, they were observed to dissolve (Fig. 2 *e*), in contrast to those maintained at room temperature (Fig. 2 *c*), confirming earlier observations (Chung et al., 1977). In a similar manner, treatment with 10 mM EDTA (in PBS) at room temperature led to a dissolution of the basement membranes, although in this case a few surviving "ghosts" (thin attenuated cores producing little phase contrast) were noted (Fig. 2 *d*). As expected, a combination of low temperature and EDTA also led to a dissolution of the basement membranes (Fig. 2 *f*), a process nearly complete within several hours of incubation. The ability of laminin ligand fragments E1′ and E4 (10 μM) to affect the integrity of the basement membranes at 37°C was also evaluated. These two components (Fig. 2, *h* and *j*) dissolved the basement membranes while albumin and P1′ (Fig. 2, *g* and *i*) had little or no effect. Fragment E1′ was the most potent agent and its effects were noticed after 1–2 h (see below). When E1′ and E4 were incubated with the basement membrane cores at room temperature, little dissolution was observed (data not shown). Thus the ligand-driven dissolution process was temperature dependent and favored by elevated temperature. The time course of basement membrane dissolution was evaluated at 37°C (Fig. 3) by counting surviving core structures in 0.2-ml optical chambers. Dissolution of half of the initial cores was achieved at 2 h with E1′ and at 7–8 h with E4. On the other hand, only about a 20% loss was observed after

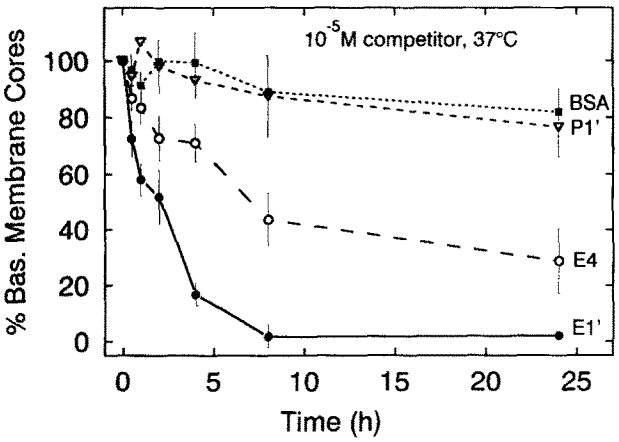

Figure 3. Time course of embryonal carcinoma basement membrane dissolution in the presence of competitive ligands. ECC basement membranes (cores of cell spherules) were incubated in TBS, 1 mM $CaCl_2$ in optical chambers at 37°C in the presence of 10 μM BSA (■, $n = 6$), P1′ (▽, $n = 3$), E4 (○, n = 7), and E1′ (●, $n = 7$). The fraction (average and standard error) of surviving cores is plotted as a function of incubation time. Laminin fragments E1′ and E4 induced a competitive dissolution of the core structures.

24 h with BSA and P1′. We attributed the considerably smaller loss here to a gradual dilutional dissociation of the laminin of the cores towards the free critical concentration. Thus the laminin-rich membranes exhibited the same characteristics as a pure laminin polymer with respect to temperature, divalent cation, and inhibiting ligands: both polymers were disrupted at 0–4°C, by chelation and by laminin fragments possessing short-arm globular domains.

To test the ability of embryonal carcinoma laminin to polymerize in vitro, basement membrane cores were isolated from cell spherules grown overnight in the presence of 50 μCi/ml [^{35}S]methionine/cysteine. The core structures were dissolved in EDTA on ice, the resultant protein solution concentrated with Aquacide, and after dialysis, incubated in TBS in 1 mM calcium chloride at 37°C. The fraction of label which aggregated was measured after centrifugation. This aggregation was found to be concentration dependent (80% aggregation at 0.5 mg/ml) and aggregation (laminin at 0.2 mg/ml) was inhibited 90% by fragment E1′ (4 μM) but not by 8 μM BSA (plots not shown).

We evaluated the embryonal carcinoma basement membranes after overnight dissolution in the cold and EDTA by EM (Fig. 4). The majority of molecular forms (88 monomers counted out of 139 laminin molecular forms), as observed in rotary shadowed Pt/C replicas, were laminin monomers with scattered dimers (19/139) and larger complexes (32/139). The latter two species were interpreted to represent incompletely dissociated complexes from the basement membrane polymer. While occasional small free globules were also noted in these replicas, no collagen was observed in agreement with earlier observations (Brauer and Keller, 1989). Although the arms of many dimers appeared tangled and of uncertain binding specificity, those dimers which were well spread out in the replicas could be divided into two categories (Fig. 4): those with contacts (interactions) between the ends of the short arms and those with contacts involving the ends of the long arms (either between pairs of

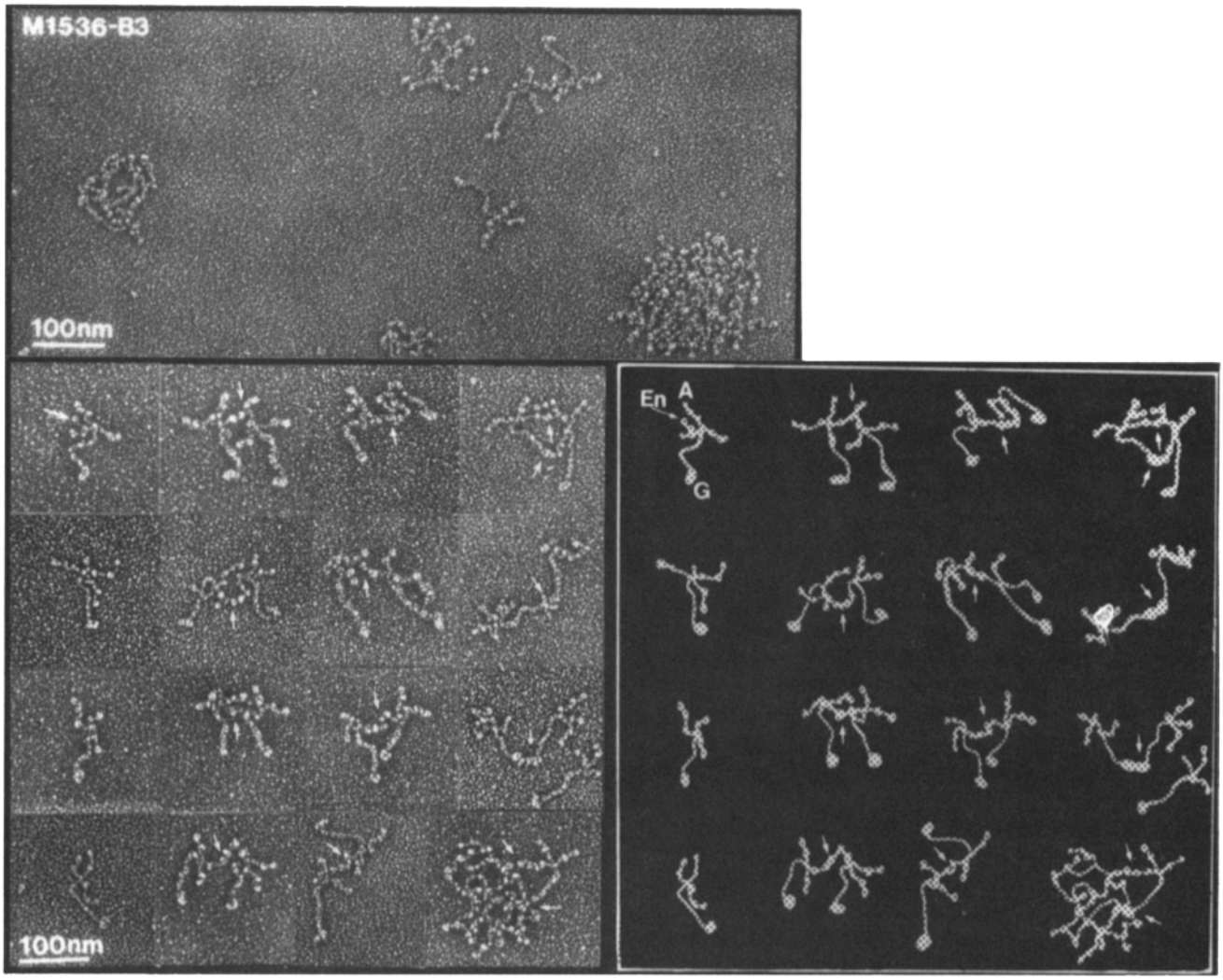

Figure 4. EM of dissociated embryonal carcinoma basement membranes. ECC M1536-B3 basement membranes were dissolved and nearly completely dissociated by incubation on ice in TBS with 1 mM EDTA. The resulting solution was prepared for low angle Pt/C rotary shadow EM as described in Materials and Methods with micrographs shown contrast reversed. Most of the molecular forms were laminin monomers with occasional larger complexes and scattered dimers (*upper panel*). Gallery of molecular dimers and one multimer shown below with interpretive drawing on right. Note (*arrows*) end–end interactions between short arms of laminin as well as some short–long and long–long associations as well. The dumbbell-shaped entactin (*En*) can be appreciated in some complexes. The longest of the "short" arms of laminin is the NH_2-terminal moiety of the A chain (*A*) and the large globule (*G*) is located at the end of the long arm.

long arms or between long arm and short arm). Short and long arm interactions could also be identified at the periphery of larger complexes (*lower right panel* of Fig. 4). These interactions are the same first observed with laminin polymers formed in vitro (Yurchenco et al., 1985) and originally, on morphological grounds, proposed as the sites for self-assembly.

Compositional Comparison of the Basement Membranes of ECC and the EHS Tumor

Embryonal carcinoma basement membranes (cores) were analyzed by SDS-PAGE (Fig. 5, lane *3*) and found to consist almost entirely of laminin (A and B chains on reduced gels) and a lesser amount of entactin. Some of the entactin, which is highly sensitive to proteolysis (Mann et al., 1988) had degraded to 120 kD. Again, no type IV collagen bands were observed. An aliquot of core material was treated overnight with heparitinase, fractionated by SDS-PAGE (Paulsson et al., 1987*b*), electro-eluted (blotted) onto nitrocellulose, blocked with BSA, incubated with a rat mAb specific for mouse heparan sulfate proteoglycan core protein (mAb HK-102, kindly provided by Dr. Koji Kimata, Nagoya University, Nagoya, Japan) and bound antibody detected with ^{125}I-protein A. Heparan sulfate proteoglycan core was detected by this method (data not shown); however, it was at such a low concentration that the band could not be detected in gels stained with Coomassie blue.

The matrix of the EHS tumor contained laminin, entactin, type IV collagen, and minor components (Fig. 5, lanes *4–8*). Bacterial collagenase degraded the collagen to small soluble species leaving behind principally laminin in the particulate fraction while 2 M guanidine-HCl selectively extracted laminin and entactin (and heparan sulfate proteoglycan as previously shown) (Yurchenco et al., 1987) leaving behind

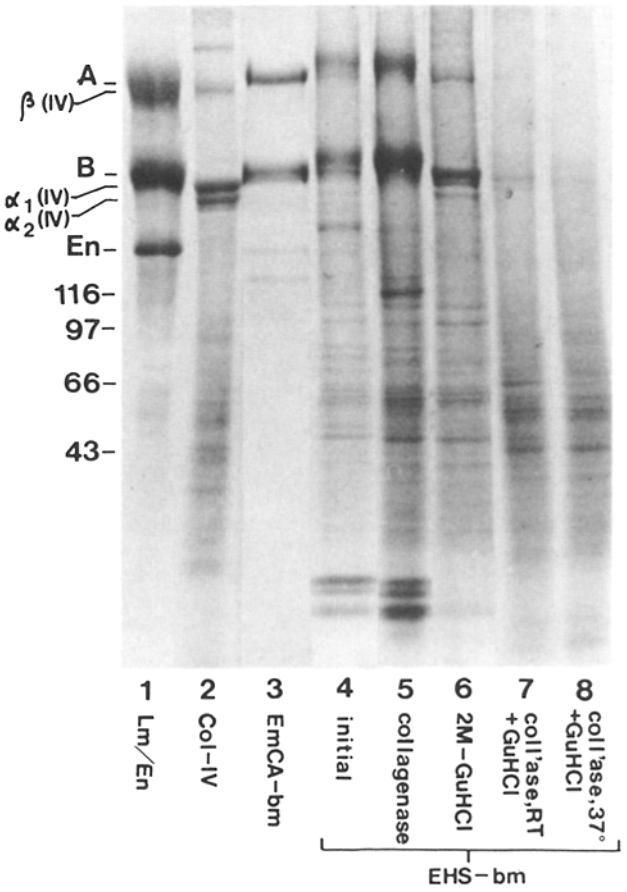

Figure 5. Comparison of basement membranes of ECC with EHS tumor. SDS-PAGE, 3.5–12% linear acrylamide gradient. All samples were electrophoresed, reduced, and stained with Coomassie blue. Samples: lane *1*, purified EHS-laminin/entactin standard; lane *2*, EHS-type IV collagen standard; lane *3*, embryonal carcinoma basement membrane cores; lane *4*, EHS matrix pellet after wash in TBS; lane *5*, EHS matrix pellet after treatment with bacterial collagenase overnight at room temperature; lane *6*, EHS matrix pellet after extraction with 2 M guanidine-HCl in TBS; lane *7*, EHS matrix pellet after treatment with both collagenase (room temp.) and 2 M guanidine-HCl; lane *8*, same as lane *7* except digestion at 37°C. Guanidine-HCl completely extracted laminin from EHS matrix leaving behind type IV collagen (5M urea and SDS extraction work equally well). Bacterial collagenase, on the other hand, degraded collagen leaving behind laminin. Little matrix residue remained after treatment of EHS tumor with both agents.

type IV collagen in the insoluble fraction. Guanidine-HCl (2 M) (Fig. 5, lanes *6–8*), 5 M urea, and 3% SDS (Figure 6 and data not shown) were found to extract the laminin to similar degrees and were used to selectively remove this component for quantitation and EM, as described below. A combination of collagenase and guanidine extraction left little remaining insoluble mass.

Laminin Pools in the EHS Basement Membrane

Nearly all laminin synthesized by the cells of the EHS tumor is found in the basement membrane (Timpl et al., 1979), a structure which accounts for half the total tumor mass (Yurchenco and Schittny, 1990). Chelation with EDTA is a standard method for the purification of laminin from this tumor (Paulsson et al., 1987*a*); however, some of the laminin remains insoluble in the residual tumor matrix. These two pools of laminin were quantitated (Fig. 6 *a*) by sequential extraction with 10 mM EDTA followed by extraction of the residue by boiling with 3% SDS-solubilizing buffer. We found that 79 ± 3% (mean ± SD, n = 17) of total laminin was extracted by EDTA with 21 ± 3% released by subsequent SDS treatment (residual pool). Subsequent boiling in SDS in the presence of reducing agent released almost no additional laminin (data not shown). When the EHS tumor was extracted with EDTA followed by 5 M urea, 23 ± 3% (n = 3) of laminin was in the urea fraction, similar to the SDS fraction. The bonds holding the two pools of laminin in the basement membrane were further explored.

Competitive Extraction of Laminin from the EHS Tumor Matrix

When washed EHS tumor matrix (particulate fraction) was incubated in buffer (TBS) at 37°C overnight, some laminin was present in the supernatant (Fig. 6 *b*). The concentration of laminin in this fraction was quantitated by gel scanning and protein assay and found to be 0.08 mg/ml (0.078 and 0.082 mg/ml, measurements of two separate samples): this value is nearly identical to the free critical concentration of laminin polymerization (0.1 mg/ml). When the EHS matrix was incubated in the same buffer on ice, a substantially larger fraction of laminin was released. EDTA released most of the EHS laminin regardless of whether incubated at 37°C or on ice. Thus laminin within the EHS tumor is similar to laminin polymerization in vitro in that the polymer state is inhibited by chelation and low temperature.

The ability of protein ligands (laminin fragments, type IV collagen and BSA) to competitively displace laminin from the EHS basement membrane was evaluated. Since the EHS basement membrane, unlike that of the ECC, possesses type IV collagen, we reasoned that in order for a competitive ligand of self-assembly to displace laminin from the EHS matrix, there must either be no other interactions anchoring laminin, or the particular ligand must in itself be capable of competing all significant interactions (both self-assembly and other anchoring bonds) that immobilize laminin. It has been proposed, for example, that entactin (nidogen) serves as a bridging molecule between laminin and type IV collagen such that the COOH-terminal globule of entactin binds to laminin and the NH_2-terminal globule of entactin binds to collagen (Aumailley et al., 1989; Fox et al., 1991).

For these experiments, the protein in the growing tumor was biosynthetically radiolabeled with [^{35}S]methionine/cysteine. We first examined the EDTA (extractable) pool of laminin by incubating washed tumor matrix with different concentrations of specific ligand. To work with type IV collagen at concentrations comparable to the other ligands, it was necessary to selectively remove the COOH-terminal globular domain as previously described (Yurchenco and Furthmayr, 1984): otherwise the collagen polymerized and precipitated at low concentrations. This pepsin-treated type IV collagen possesses all of the collagenous regions proposed previously as binding sites (bridging sites) for laminin (Charonis et al., 1985) or for entactin (Aumailley et al., 1989). The fractions were evaluated in Coomassie blue–stained SDS–polyacrylamide gels and in fluorograms (Fig. 7), and quantitated (Fig. 8). The Coomassie blue–stained

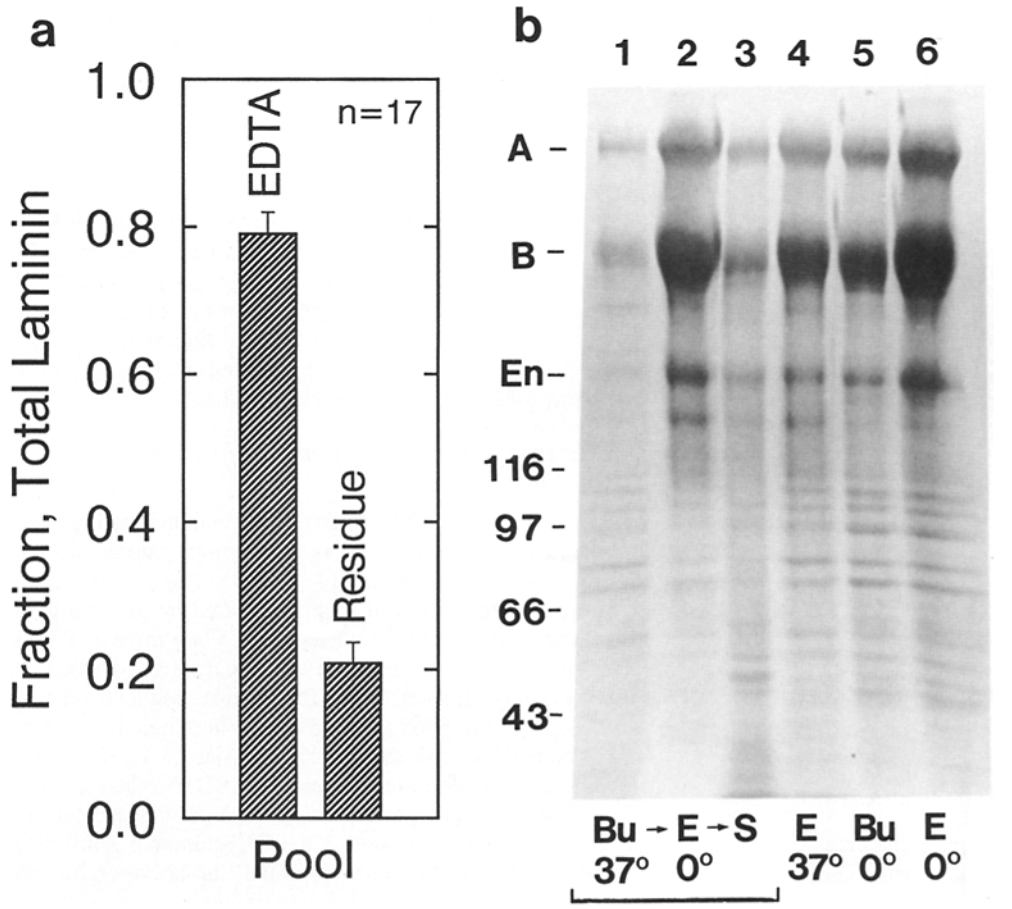

Figure 6. Laminin pools present in the EHS tumor matrix. (*a*) EHS matrix, biosynthetically labeled with [^{35}S]methionine/cysteine, was incubated in multiple aliquots with 10 mM EDTA in TBS buffer for several hours at 0–5°C and centrifuged to remove the pellet (supernatant contains the EDTA laminin pool). The insoluble matrix residue was then boiled in 3% SDS buffer and centrifuged (remaining supernatant contains the residue pool). The sizes (mean ± SD) of these pools were determined by quantitation of radioactivity in the A and B bands of laminin after SDS-PAGE. (*b*) SDS-PAGE (Coomassie blue-stained 3.5–12% gradient gels, reduced) analysis of laminin extracts (total supernatants) from EHS tumor sequentially extracted with TBS (*Bu*, buffer; lane *1*), 10 mM EDTA on ice (*E*, 0°C; lane *2*), and then SDS (*S*, boiled; lane *3*). Only a small fraction of laminin (the free critical concentration) was released by buffer. EDTA removed most of the laminin either in the cold (lane *6*) or at 37°C (lane *4*). When tumor matrix was incubated with buffer on ice (lane *5*), substantial laminin was extracted. Thus laminin was dissociated from the EHS basement membrane by both EDTA and low temperature, two conditions which also inhibit polymerization in vitro.

gels revealed both the protein released from the EHS tumor as well as the ligand added. The fluorograms revealed only the basement membrane proteins (labeled) released into solution. Incubation with fragment E1′ or E4 released a substantial amount of laminin (with entactin) as compared with albumin, collagen IV (pepsin treated), or P1′ (Fig. 7, compare band intensities of A and B chains in lanes *1* [E1′] and *10* [E4] with those in lanes *19*, *22*, and *25*). Furthermore, the ratios between ligand-extracted and subsequent EDTA-extracted laminin chains changed as a function of E1′ or E4 concentration (but not P1′, Col-IVp, or BSA) such that the greater the ligand concentration, the more laminin solubilized by the ligand and the less laminin left to be subsequently extracted by EDTA (Fig. 7, compare E1′ lanes *1* and *2* with lanes *7* and *8* and compare E4 lanes *10* and *11* with lanes *16* and *17*).

Scintillation spectroscopy of the laminin A and B bands was used for quantitation. The fraction of the EDTA pool released into solution by a given ligand was calculated from the amount of laminin (radioactivity in A and B chain bands) released by ligand divided by that amount plus the additional laminin released by EDTA. Laminin fragments E1′ and E4 were found to selectively release laminin (with associated entactin chain) from the EHS matrix in a concentration-dependent fashion. The time course of this selective laminin displacement was evaluated with fragment E1′ using 15 μM ligand at 37°C. Relative to the amount of laminin released into solution after 28 h, it was found (plot not shown) that by 1 and 8 h, 42 and 84% were displaced, respectively. The rate of change decreased considerably after that time such that a near-plateau (97%) was achieved by 23 h (overnight condition). Therefore, we concluded that overnight incubation with competitive ligand represented a condition approaching equilibrium.

In contrast, the levels of laminin released in the presence of fragment P1′, type IV collagen, and BSA remained the same as buffer alone after overnight incubations and did not increase as a function of concentration (Fig. 8). Thus the same laminin fragments which possess short arm globular domains and which inhibit laminin polymerization and dissolve embryonal carcinoma basement membranes competitively extract laminin from the EDTA pool. The fraction extracted at 15 μM exceeded 50% and had not reached a plateau at that concentration: from this we concluded that even larger fractions would be extracted at higher concentrations. It is likely, based on the shape of the curve (Fig. 8 *a*), that all of the EDTA laminin pool can be selectively extracted by these ligands at sufficiently high ligand/EHS ratios.

The residual laminin pool which remained after extraction with EDTA was similarly examined (Fig. 9). When this matrix was directly incubated with fragments E1′, E4, and BSA (Fig. 9, *a* and *b*) the pool was resistant to ligand extraction:

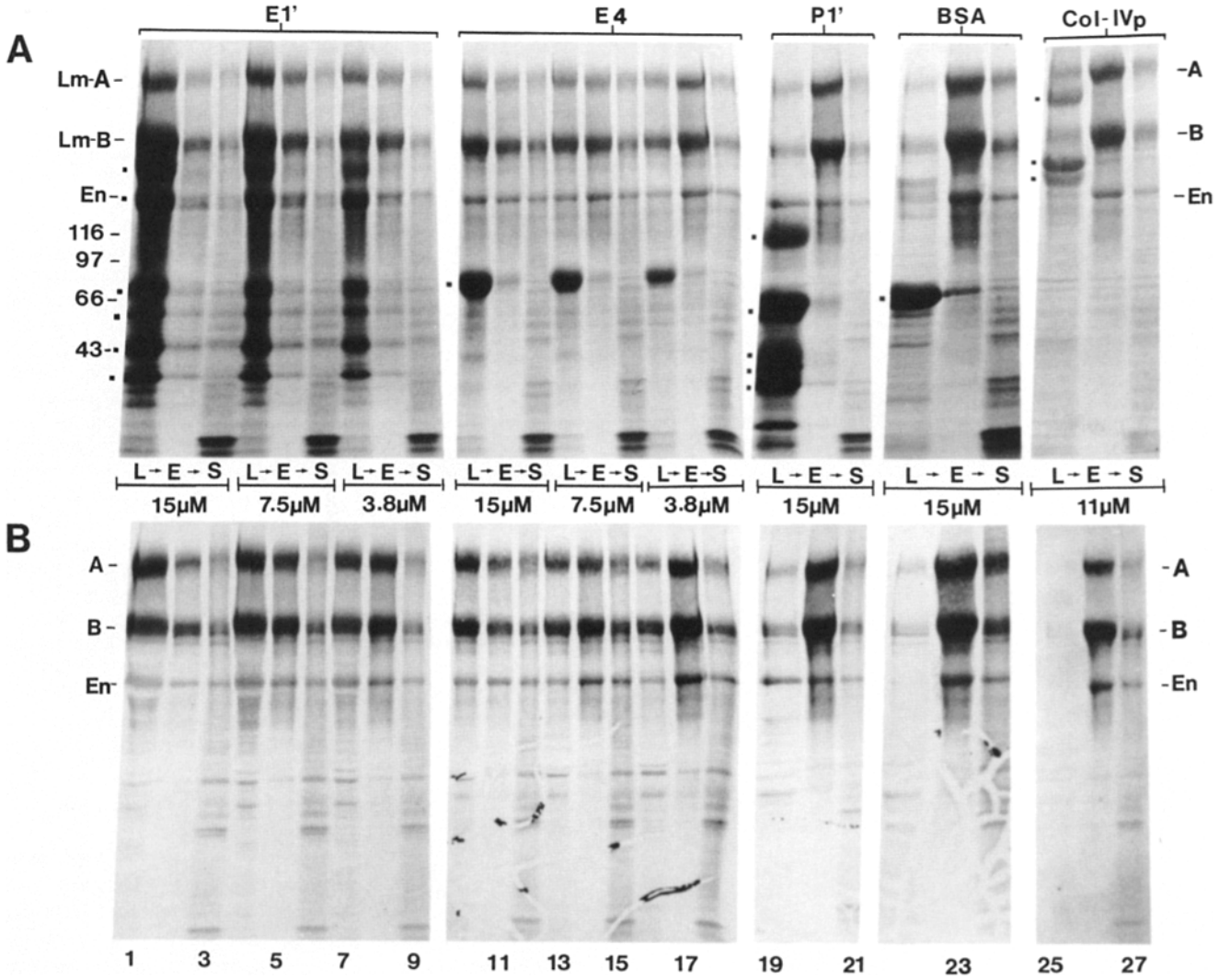

Figure 7. Competitive ligand extraction of EDTA laminin pool of the EHS basement membrane. Aliquots of particulate ^{35}S-amino acid–labeled EHS matrix were incubated sequentially with ligand (*L*) at the indicated final concentrations, then 10 mM EDTA (to extract remainder of EDTA pool) in TBS at 5°C (*E*), and finally 3% SDS buffer (*S*). After centrifugation, the supernatants were fractionated by SDS-PAGE under reducing conditions, the gels stained with Coomassie blue (*A*) and evaluated by fluorography (*B*). The dye-stained gels revealed both extracted protein and added ligand (major bands of each ligand identified with small square dot to left of bands) while the fluorograms revealed only the protein extracted from the matrix. E1′ and E4 released substantial laminin from the matrix, especially at higher concentrations. On the other hand, P1′, BSA, and type IV collagen released little laminin (comparable with buffer levels).

only E1′ extracted any laminin above baseline at 15 μM. If, on the other hand, the residual matrix was first treated overnight with bacterial collagenase and then incubated with ligand (Fig. 9, *c* and *d*), then both E1′ and E4, in contrast to BSA, displaced laminin into solution in a concentration-dependent manner. Again, plateau was not achieved at the highest concentration evaluated. We concluded that laminin of this residual pool is not only bound to itself into a polymer, but is also bonded directly, or indirectly, to the type IV collagen scaffolding of this basement membrane. Only if the collagen scaffolding were first digested was it possible to quantitatively displace laminin into solution. The observation that E1′, but not E4, could release some laminin from the untreated pool at higher concentrations suggests that E1′ not only inhibits self-assembly, but can also, to some degree, compete against other bonds that anchor laminin to the remaining basement membrane collagen. One possibility is that E1′ can also compete against bridging bonds: fragment E1′, in contrast to E4, possesses some entactin determinants (Mann et al., 1988) and it has been reported that E1′ can bind to type IV collagen through the entactin determinants (Aumailley et al., 1989). While entactin bridging of laminin to collagen may contribute to laminin anchorage in the residual pool, other mechanisms may contribute as well.

Molecular Architecture

High angle platinum/carbon metal replication of freeze deep-etched preparations was used to study the supramolecular organization of laminin polymer, of laminin-based basement membrane of ECC and basement membrane of the EHS tumor. For these studies we used laminin polymers maintained in a buffer (TBS or PBS) of physiological ionic

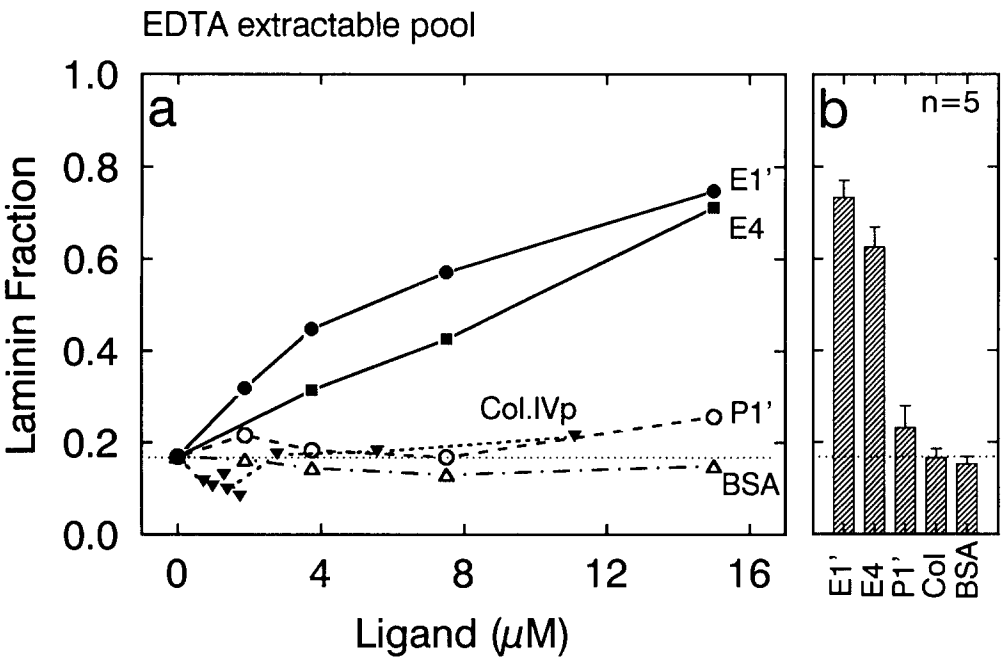

Figure 8. Concentration dependency of competitive ligand extraction of the EDTA laminin pool of EHS matrix. (*a*) Washed EHS tumor matrix was incubated overnight at 37°C in TBS containing 1 mM $CaCl_2$ with laminin fragments E1′, E4, P1′, type IV collagen lacking globular domains (*Col.IVp*), and BSA or buffer alone at the indicated concentrations. After centrifugation and a buffer wash, the residue was extracted with 10 mM EDTA in TBS for several hours at 5°C. The supernatants were analyzed by SDS-PAGE and the extracted laminin quantitated from the radiolabeled laminin in the A and B bands. The fraction of laminin liberated into solution is the ratio of ligand-extracted laminin divided by ligand-extracted laminin plus EDTA-extracted laminin. (*b*) The average (± SE) of five separate determinations at the highest ligand concentration (15 μM for E1′, E4, P1′, and BSA and 11 μM for Col-IVp) is shown in the bar graph. Both short arm fragments E1′ and E4, which specifically inhibit laminin polymerization, were observed to competitively displace laminin into solution from tissue in a concentration-dependent fashion while the short arm fragment P1′ (lacking globular domains), the threadlike domain of type IV collagen and albumin failed to release laminin above the level of buffer alone (free critical concentration).

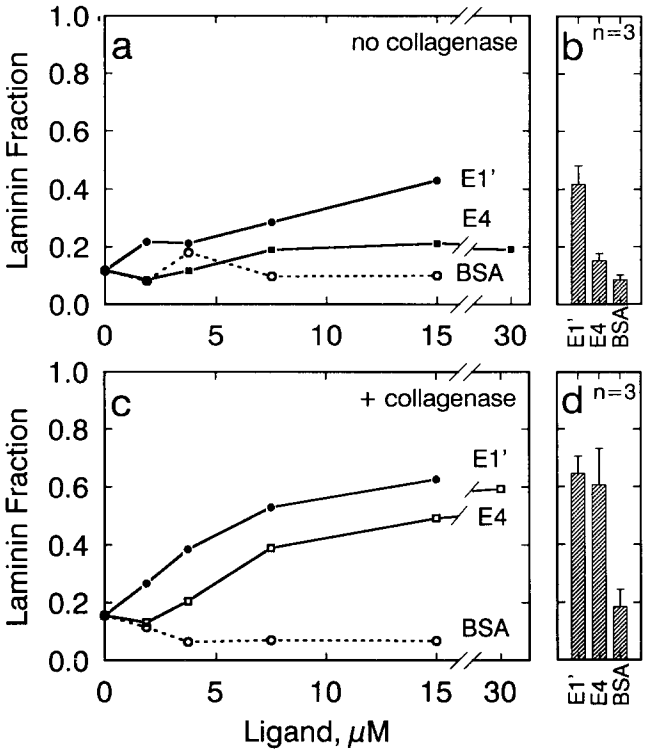

Figure 9. Quantitation of competitive ligand extraction of the residual laminin pool of EHS matrix. (*a* and *c*) The EHS matrix was first extracted with 10 mM EDTA in the cold to remove the EDTA pool. The residual matrix was divided into two aliquots: the first was maintained at 37°C overnight (*a*, no collagenase) while the second was digested with bacterial collagenase under the same conditions (*c*). The two preparations were then mixed with different concentrations of ligand (*E1′*, *E4*, and BSA), incubated overnight in TBS containing 1 mM $CaCl_2$ at 37°C, centrifuged, re-extracted with buffer, and the final residue was boiled with SDS Laemmli solubilizing buffer to remove any remaining laminin. The fraction of laminin liberated from the residual pool is the ligand extracted laminin divided by the ligand extract plus the SDS extracted laminin (determined from the A and B bands of laminin after SDS-PAGE). (*b* and *d*) The average (± SE) for three separate determinations at 15 μM ligand is shown in the bar graphs for the residual pool not treated with collagenase (*b*) and after collagenase incubation (*d*). Fragment E4 quantitatively released laminin into solution only if first treated with collagenase. E1′ released some laminin without collagenase treatment, a fraction which nonetheless substantially increased with collagenase. Thus laminin of the residual pool is linked not only to itself, but to the type IV collagen network as well.

strength. Rotary replication (1.0–1.2 nm application) was used for this study.

The basement membrane (cores) and reconstituted laminin polymer gels were examined by this method (Fig. 10). The etched surfaces for these two samples were quite similar and revealed extensive arrays of what can be described as interconnecting "struts". These struts were connected each to two to three neighboring struts to form a three-dimensional network. In the ECC replica, network regions suggestive of honeycombs were observed. Small globules of several sizes (6–8 and ~20 nm metal-coated diameters) could be identified as part of these structures and might correspond to the short and long arm globules. At higher magnification, better structural resolution was observed with the purified laminin polymer (Fig. 10 *c*). Stereo pairs were examined with a

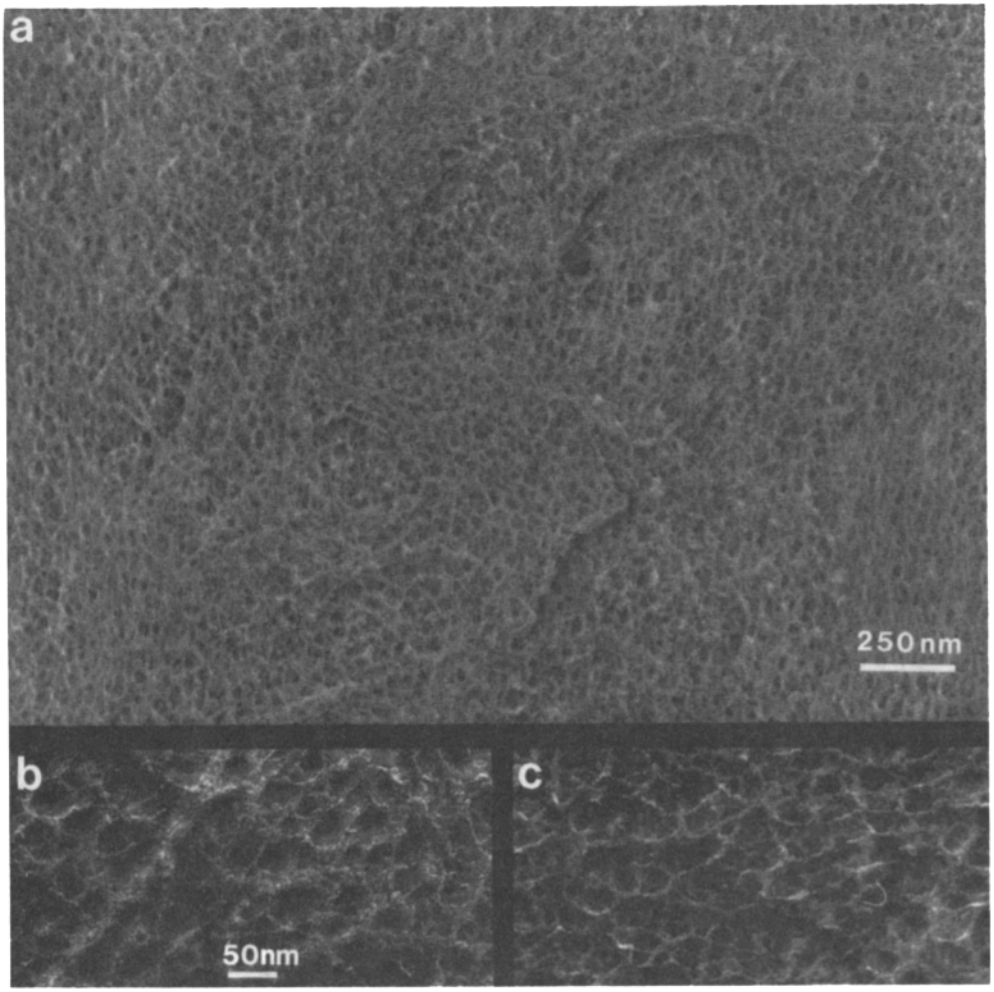

Figure 10. EM of ECC basement membrane laminin. ECC basement membrane cores (*a* and *b*) and thermally gelled purified laminin (*c*) (3.5 mg/ml in TBS, 1 mM $CaCl_2$) were frozen in propane, fractured, and deep etched in a Balzers BAF500K unit, rotary shadowed at high angle (45°C) with 1 nm Pt/C below liquid nitrogen temperatures, backed with carbon, and the replicas freed of tissue and examined in the electron microscope. The structure can be characterized for both ECC basement membrane and laminin gel as a quasi-regular mesh array of interconnecting (and somewhat flexible) struts. The ECC struts measured 28 ± 9 nm (average and standard deviation with $n = 300$ measurements) while the reconstituted laminin polymer struts measured 31 ± 8 nm ($n = 300$ measurements). At higher magnification small globules could often be appreciated as an integral part of the network.

stereoscope: 300 struts from each network, whose axes were near the axis of the horizon, were measured. The ECC struts measured 28 ± 9 nm (average and standard deviation with $n = 300$ measurements) while the reconstituted laminin polymer struts measured 31 ± 8 nm ($n = 300$ measurements).

The EHS tumor matrix was similarly examined (Fig. 11) following homogenization into small particles to permit washing the matrix largely free of cellular contents (as gauged by SDS-PAGE) and to permit the application of thin coats of sample material between the copper planchets for vitreous freezing. The washed EHS meshwork (Fig. 11 *a*) was noted to be a tight network of branching filaments and struts and spaces ranging from 5 to 25 nm. When the collagen was removed from the EHS matrix by collagenase digestion (Fig. 4), the replicated network array (Fig. 11 *b*) was observed to be a quasi-regular array of interconnecting struts, highly similar to that shown in Fig. 10. We have concluded that the network observed is that of laminin for the following reasons: First, laminin is the major protein species present in the EHS matrix after collagenase treatment and washing (Fig. 4): most of the other proteins are of small molecular weight, below the resolution of the technique. Second, the network is nearly identical to that observed with a purified laminin gel (Fig. 10) and quite distinct from the only other polymer identified in the EHS tumor, the type IV collagen network. On the other hand, the network remaining after extraction of laminin with guanidine–HCl (Fig. 11 *c*) was essentially identical to the type IV collagen network described previously and confirmed as type IV collagen with gold-tagged antibody (Yurchenco and Ruben, 1988). It consisted of branching filaments and integral globular domains. The branchings have previously been shown to be formed by the lateral associations of individual triple helical monomers (Yurchenco and Ruben, 1987; Yurchenco and Ruben, 1988). While the network of laminin is composed largely of interconnecting flexible struts, measuring on average 30 nm in length, the branching filaments of type IV collagen are more variable in length (with an asymmetrical length distribution) and more variable in diameter, the latter resulting from the joining of different numbers of triple helical segments (Yurchenco and Ruben, 1987, 1988).

Discussion

The data of this study support the hypothesis that laminin is a major network polymer in basement membranes and is largely independent and free-standing. Laminin self-assembly was first characterized in vitro with purified protein (Yurchenco et al., 1985) and the arguments for the structural

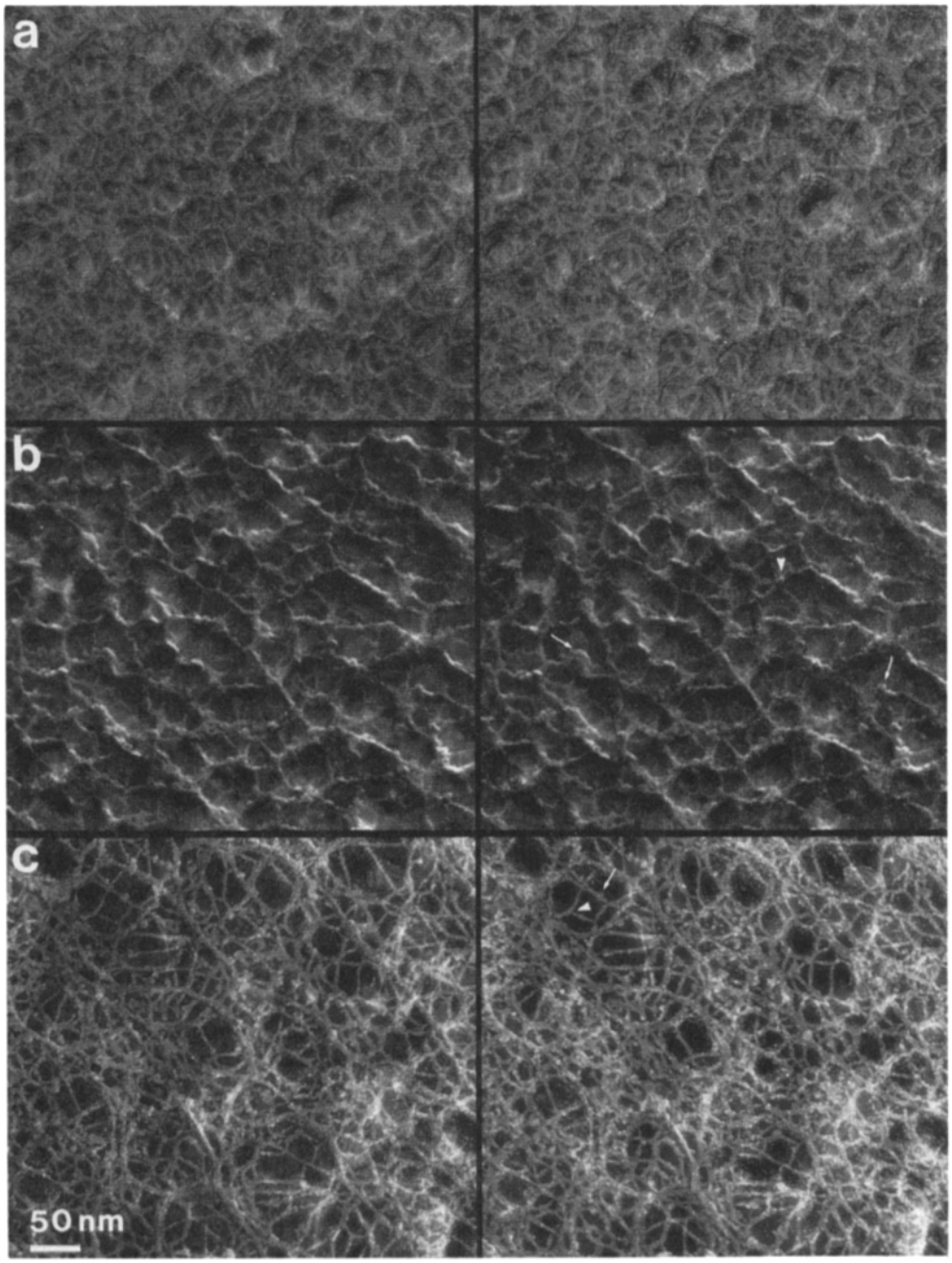

Figure 11. EM of EHS tumor basement membrane. The EHS tumor matrix was vitreous frozen, fractured, deep etched, and rotary replicated with 1.2 nm Pt/C at high angle (60°) either untreated (*a*), after removal of type IV collagen by incubation overnight at room temperature with bacterial collagenase to reveal the laminin polymer (*b*), or after removal of laminin by extraction with 2 M guanidine-HCl in TBS to expose the type IV collagen network (*c*). Electron micrographs are shown as stereo pairs, contrast reversed. The collagenase-treated tissue (*b*) is of similar architecture to the purified laminin gel shown in the preceding figure while the guanidine-treated tissue (*c*) is essentially the same collagenous network as previously described in detail (Yurchenco and Ruben, 1988). Arrowhead in *b* indicates joining of struts or lateral fusion of filaments while small arrows indicate globules in network. The tighter mesh of laminin/collagen network (*a*) is likely formed by intermeshing of laminin (*b*) and collagen polymers (*c*).

relevance of the laminin polymer in tissues were inconclusive. In the present study, both biochemical and morphological lines of investigation were pursued to evaluate laminin in basement membranes formed by two types of cells and the results were complimentary. The biochemical evidence is that both reconstituted polymers and cell-formed polymers are temperature- and divalent cation-dependent and that the bonds between laminin molecules in tissue, just as in reconstituted polymers, are specifically inhibited and dissociated by fragments possessing short arm globule domains. The morphological evidence is that a similar laminin network can be visualized in reconstituted polymers, embryonal carcinoma basement membranes, and EHS basement membranes. Moreover, these polymer networks are distinct from the network of type IV collagen. Given that laminin/entactin and type IV collagen are, on a mass basis, the major components of the EHS tumor matrix as well as other basement membranes and that these two components are the only basement membrane components known to polymerize, it is likely that laminin/entactin, alone or with type IV collagen defines the basic scaffold structure of basement membranes.

Mechanism of Basement Membrane Formation

Since we find that laminin, as a purified component, will assemble into the same polymer as that found in the basement membrane formed by cells and found in tissue, it follows that the basic information for correct three-dimensional architecture is encoded in the laminin monomer itself. These data then strongly favor the hypothesis that the supramolecular

organization of the laminin, like that of type IV collagen (Yurchenco and Ruben, 1987), is created through mass action-driven self-assembly; i.e., a cell need only secrete the required laminin protomers, with or without type IV collagen protomers, at appropriate concentrations into a diffusion-limited space to create a functional architecture. In the case of the ECC, the outer cell layer forms this diffusion barrier while in the EHS tumor the barrier is formed by the cell membranes of the tumor islands and the outer capsule. Given this basic concept, we recognize that the tissue environment of these components can nevertheless influence assembly and structure. For example, there is evidence that heparin can modulate laminin polymerization at biological concentrations (Yurchenco et al., 1990) and that the critical concentration of laminin is lowered on lipid bilayer surfaces and may play a role in favoring polymer propagation off of the cell membrane (Kalb and Engel, 1991).

Molecular Architecture of Laminin

From rotary shadowed replicas of dissociated polymers, interactions between the outer (NH_2-terminal) globules of the short arms have been observed. In such glycerol spreads, the contour distances between pairs of short arm–bound laminin have consistently been about two arm lengths, suggesting little overlap. The importance of short arm globular interactions are supported by biochemical studies in which it has been shown that fragment E4 (domains VI and V of the B1 chain) and E1′ (short arm complex with A and B2 chain short arm globules), but not P1′ (short arm complex possessing EGF-like domains but lacking inner and outer globules) inhibit polymerization. We have further found that E4 binds directly to E1′ in a calcium-dependent manner (Schittny, J. C., and P. D. Yurchenco. 1989. *J. Cell Biol.* 109:44 abstr.). Since P1′ lacks both outer and inner globules we cannot rule out, on biochemical grounds alone, the participation of A and B2 chain inner globules (domain IV) in polymerization. Furthermore, the importance of long arm interactions remain uncertain. Rotary shadowed replicas reveal associations of the long arm globule (G domain) and between G and the short arm termini. Although isolated fragment E3 is capable of dimerization (Yurchenco et al., 1990), fragments E3 and E8 (containing contiguous moieties of the long arm globule) have not been found to inhibit laminin polymerization and, at the concentrations evaluated, have not been observed to interact with immobilized laminin by affinity chromatography (P. Yurchenco, unpublished observations). It has also been observed (Bruch et al., 1989) that a large cathepsin G fragment of laminin, consisting of all three arms, undergoes a calcium-dependent precipitation while the long arm fragment does not and remains in solution. Since interactions involving the short arms have not been measured biochemically, they may be of quite low affinity and make relatively minor contributions to the network.

The visualization of polymer replicas with ~30 nm flexible struts meeting at vertices with two to three other struts is compatible with a model in which each short arm (flexible and elastic structures measuring on average 37 nm in low angle glycerol spreads) joins with two other short arms to produce a polymer: this presumes a reduction (~10%) in short arm dimensions relative to that observed in glycerol spreads and is consistent with a reduction of the D periodicity observed for interstitial collagen examined in deep-etched replicas [Yurchenco and Ruben, 1987]. The model, to be compatible with the single arm lengths and the polymer struts, requires that each arm bind to at least two other short arms; otherwise, the struts would be twice the length of each short arm. Fragment E1′ binds to itself (Paulsson et al., 1988) and we have observed dimers and smaller numbers of trimers of E1′ in glycerol spreads (P. Yurchenco, unpublished observations) in which there are interactions between the ends of the A-chain short arms: the trimers are formed by one arm from each molecule meeting at a single vertex. Struts the length of the long arm (~75 nm), 25% of all laminin arms, are infrequently observed in the polymer replicas. It may be that in a tight mesh of short arms, the long arms are obscured because of nonbinding overlaps of long arms; i.e., we do not have the necessary resolution to discriminate between true bonds and overlapping crossovers. Thus it will clearly take further experimentation, (e.g., site-specific antibody decoration of the different domains of laminin in the polymer) to definitively solve the three-dimensional structure. For the present we can only propose a tentative model (working hypothesis) consistent with the data (Fig. 12).

Laminin Anchorage to Type IV Collagen

While all, or nearly all, laminin is immobilized through self-interactions, one-fifth of laminin is also anchored to type IV collagen in the EHS basement membrane. This binding could be direct (Charonis et al., 1985) or indirect through a bridging molecule. One strong candidate for a bridging molecule is entactin which has been shown to bind in vitro at one of its NH_2-terminal globules to two sites along the triple helical domain of type IV collagen and at its COOH-terminal globule to laminin (Aumailley et al., 1989; Fox et al., 1991). The molar concentrations of laminin and type IV collagen and entactin are roughly equal in the EHS tumor (see Yurchenco and Schittny, 1990). If the predominant cross-link is direct or via an anchoring molecule such as entactin in stoichiometric equivalency, then there may be an imbalance of binding sites in laminin and collagen because 80% of the collagen binding sites are inaccessible to bridging bonds. In particular, the sites on collagen may be sterically buried through lateral associations between collagenous segments or otherwise constrained by immobilization in a network. In the case of bridging molecules in low stoichiometric amount, we could explain the heterogeneity by simply an insufficiency of such molecules.

Structural and Functional Heterogeneity

In general, structural diversity in different basement membranes may be created by variations in the ratios of major components, by genetic isoform substitutions of laminin and collagen, by variations in posttranslational modification, and by the presence of site-specific components. In this study, we have identified heterogeneity both between basement membranes (compositional heterogeneity) as well as within a single basement membrane in which only a fraction of laminin is bridged to collagen.

Since we find a similar laminin architecture in either a pure reconstituted gel or a cell-formed scaffolding, and since previous studies have shown that pure reconstituted type IV collagen polymers are nearly identical to those found in tissue (Yurchenco and Ruben, 1988), it follows that each can

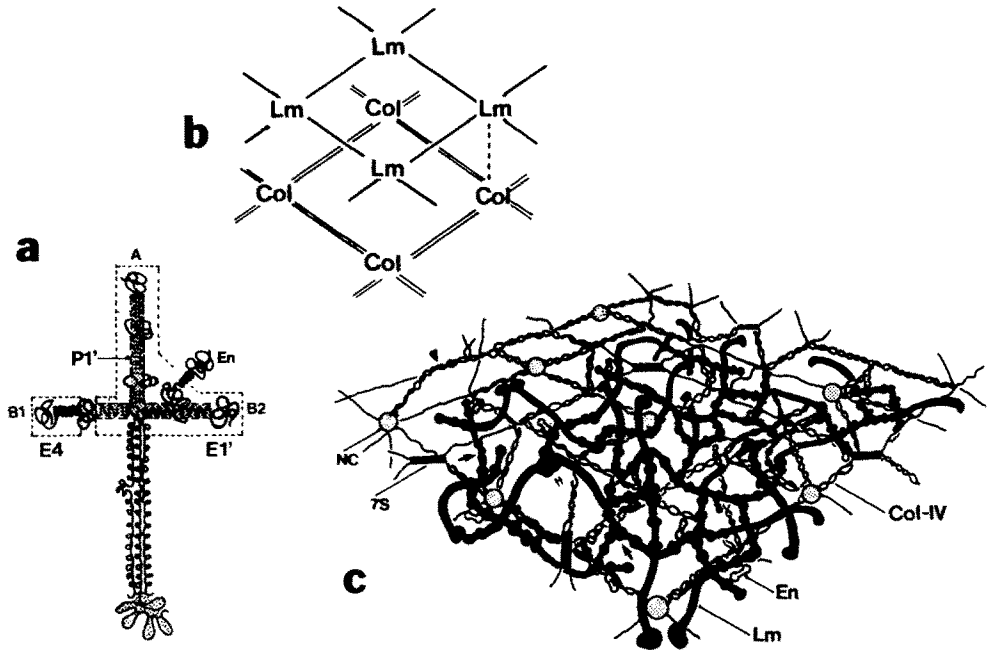

Figure 12. Laminin model. (*a*) Three chain structure of laminin molecule (see Beck et al., 1990) showing correspondence between domains and laminin fragments. (*b*) Highly schematic model of a basement membrane scaffold revealing two separate polymer networks of laminin (*Lm*) and type IV collagen (*Col*) in which 20% of laminin molecules are linked (—) to the covalently stabilized network of type IV collagen. (*c*) A more detailed working model for the laminin/type IV collagen double polymer basement membrane scaffolding principally held together by short arm globular interactions (*arrows*). A more stable covalently cross-linked type IV collagen network composed of lateral (*arrow head*), NH_2-terminal (*7S*) and COOH-terminal (*NC*) bonds forms independently. Strong but noncovalent bridges form between 20% of total laminin and collagen: these could be formed directly, through entactin/nidogen (*En*) or other components.

form a correct polymer independent of the other. This independence should permit a basement membrane scaffolding to be formed with any ratio of the two components. Laminin or laminin variants are generally found associated with type IV collagen. However, several embryonic (e.g., blastula) (Lievo et al., 1980; Cooper and MacQueen, 1983) and newly formed (capillary bud) (Form et al., 1986) basement membranes lack type IV collagen when first formed. Given that the laminin polymer is reversible while the type IV collagen polymer is not, laminin-based basement membranes that lack type IV collagen may be better suited for the rapid remodeling of tissue that occurs in development and in conditions of regeneration and repair. In contrast, type IV collagen may be best suited in tissues of greater stability when there is need of structural support and biomechanical strength. Recently it has been reported that transglutaminase, in vitro, can cross-link laminin and entactin (Aeschlimann and Paulsson, 1991) and transglutaminase antigen can be found in several basement membranes. If this cross-linking mechanism operates in vivo, laminin would likely lose its reversibility in certain tissues. This has been proposed as another mechanism to stabilize laminin in mature tissues.

The Double Polymer Scaffolding of Complex Basement Membranes

We have presented evidence that a basement membrane scaffolding can be a single laminin polymer or a laminin–type IV collagen double polymer. In double-polymer basement membranes, it is likely that the two polymers are enmeshed. Each is formed from highly asymmetrical and flexible molecules which, because of the nature of the end–end (laminin) and lateral interactions (collagen), form porous networks. The spaces of each network would allow the laminin struts and collagen filaments to interweave during assembly (Fig. 12). Entactin (which is normally associated with laminin) would bind accessible collagen domains providing further stabilization for a fraction of laminin. Other components might participate in bridging as well. This double polymer would then serve as a substrate for interactions with other components such as heparan sulfate proteoglycan and BM-40. Such a double polymer scaffolding would have unique functions such as providing a mesh with sufficiently tight porosity to exclude mid to large macromolecules as is observed with the glomerular basement membrane filtration barrier. We note that the spaces created between the laminin–collagen double polymer of the EHS tumor appear to be in the right size range for the "pore" size of ~9 nm proposed for the glomerulus (Farquhar, 1981), in contrast to the larger spaces of the individual polymers.

We would like to thank Mrs. Barbara Hartman for her technical assistance and Drs. Jules O'Rear and Robert Trelstad for their helpful discussions and advice (all from Robert Wood Johnson Medical School).

This study was supported by grant RO1-DK36425 from the National Institutes of Health.

Received for publication 27 January 1992 and in revised form 17 March 1992.

References

Aeschlimann, D., and M. Paulsson. 1991. Cross-linking of laminin-nidogen complexes by tissue transglutaminase: a novel mechanism for basement membrane stabilization. *J. Biol. Chem.* 266:15308–15317.

Aumailley, M., H. Wiedemann, K. Mann, and R. Timpl. 1989. Binding of nidogen and the laminin–nidogen complex to basement membrane collagen type IV. *Eur. J. Biochem.* 184:241–248.

Beck, K., I. Hunter, and J. Engle. 1990. Structure and function of laminin: anatomy of a multidomain glycoprotein. *FASEB (Fed. Am. Soc. Exp. Biol.) Monogr. J.* 4:148–160.

Brauer, P. R., and J. M. Keller. 1989. Ultrastructure of a model basement membrane lacking type IV collagen. *Anat. Rec.* 223:376–383.

Bruch, M., R. Landwehr, and J. Engel. 1989. Dissection of laminin by cathepsin G into its long and short arm structures and localization of regions involved in calcium dependent stabilization and self-association. *Eur. J. Biochem.* 185:272–279.

Carlin, B., R. Jaffe, B. Bender, and A. Chung. 1981. Entactin, a novel basal lamina-associated sulfated glycoprotein. *J. Biol. Chem.* 256:5209–5214.

Charonis, A. S., E. C. Tsilibary, P. D. Yurchenco, and H. Furthmayr. 1985. Binding of laminin to type IV collagen: a morphological study. *J. Cell Biol.* 100:1848–1853.

Chung, A. E., I. L. Freeman, and J. E. Braginski. 1977. A novel extracellular membrane elaborated by a mouse embryonal carcinoma-derived cell line. *Biochem. Biophys. Res. Commun.* 79:859–868.

Cooper, A. R., and H. A. MacQueen. 1983. Subunits of laminin are differentially synthesized in mouse eggs and early embryos. *Dev. Biol.* 96:467–471.

Dziadek, M., and R. Timpl. 1985. Expression of nidogen and laminin in basement membranes during mouse embryogenesis and in teratocarcinoma cells. *Dev. Biol.* 111:372–382.

Dziadek, M., M. Paulsson, and R. Timpl. 1985. Identification and interaction repertoire of large forms of the basement membrane protein nidogen. *EMBO (Eur. Mol. Biol. Organ.) J.* 4:2513–2518.

Farquhar, M. G. 1981. The glomerular basement membrane: a selective macromolecular filter. *In* Cell Biology of Extracellular Matrix. E. D. Hay, editor. Plenum Press, New York. 335–378.

Form, D. M., B. M. Pratt, and J. A. Madri. 1986. Endothelial cell proliferation during angiogenesis. *Lab. Invest.* 55:521–530.

Fox, J. W., U. Mayer, R. Nischt, M. Aumailley, D. Reinhardt, H. Wiedemann, K. Mann, R. Timpl, T. Krieg, J. Engel, and M.-L. Chu. 1991. Recombinant nidogen consists of three globular domains and mediates binding of laminin to collagen type IV. *EMBO (Eur. Mol. Biol. Organ.) J.* 10:3137–3146.

Fujiwara, S., H. Shinkai, R. Deutzmann, M. Paulsson, and R. Timpl. 1988. Structure and distribution of N-linked oligosaccharide chains on various domains of mouse tumor laminin. *Biochem. J.* 252:453–461.

Kalb, E. and J. Engel. 1991. Binding and calcium-induced aggregation of laminin onto lipid bilayers. *J. Biol. Chem.* 266:19047–19052.

Laemmli, U. K. 1970. Cleavage of structural proteins during the assembly of the head of bacteriophage T4. *Nature (Lond.).* 227:680–685.

Lievo, I., A. Vaheri, R. Timpl, and J. Wartiovaara. 1980. Appearance and distribution of collagens and laminin in the early mouse embryo. *Dev. Biol.* 76:100–114.

Mann, K., R. Deutzmann, and R. Timpl. 1988. Characterization of proteolytic fragments of the laminin-nidogen complex and their activity in ligand-binding assays. *Eur. J. Biochem.* 178:71–80.

Paulsson, M. 1988. The role of Ca^{2+} binding in the self-aggregation of laminin-nidogen complexes. *J. Biol. Chem.* 263:5424–5430.

Paulsson, M., and K. Saladin. 1989. Mouse heart laminin: Purification of the native protein and structural comparison with Engelbreth-Holm-Swarm tumor laminin. *J. Biol. Chem.* 264:18726–18732.

Paulsson, M., K. Saladin, and R. Landwehr. 1988. Binding of Ca^{2+} influences susceptibility of laminin to proteolytic digestion and interactions between domain-specific laminin fragments. *Eur. J. Biochem.* 177:477–481.

Paulsson, M., K. Saladin, and E. Engval. 1991. Structure of laminin variants: the 300-kDa chains of murine and bovine heart laminin are related to the human placental merosin heavy chain and replace the A chain in some laminin variants. *J. Biol. Chem.* 266:17545–17551.

Paulsson, M., M. Aumailley, R. Deutzmann, R. Timpl, K. Beck, and J. Engel. 1987*a*. Laminin-nidogen complex: extraction with chelating agents and structural characterization. *Eur. J. Biochem.* 166:11–19.

Paulsson, M., P. D. Yurchenco, G. C. Ruben, J. Engel, and R. Timpl. 1987*b*. Structure of low density heparan sulfate proteoglycan isolated from a mouse tumor basement membrane. *J. Mol. Biol.* 197:297–313.

Schittny, J. C., and P. D. Yurchenco. 1990. Terminal short arm domains of the basement membrane protein laminin are critical for its self-assembly. *J. Cell Biol.* 110:825–832.

Timpl, R. 1989. Structure and biological activity of basement membrane proteins. *Eur. J. Biochem.* 180:487–502.

Timpl, R., H. Rohde, P. G. Robey, S. I. Rennard, J.-M. Foidart, and G. R. Martin. 1979. Laminin - a glycoprotein from basement membranes. *J. Biol. Chem.* 254:9933–9937.

Yurchenco, P. D., and H. Furthmayr. 1984. Self-assembly of basement membrane collagen. *Biochemistry.* 23:1839–1850.

Yurchenco, P. D., and G. C. Ruben. 1987. Basement membrane structure in situ: evidence for lateral associations in the type IV collagen network. *J. Cell Biol.* 105:2559–2568.

Yurchenco, P. D., and G. C. Ruben. 1988. Type IV collagen lateral associations in the EHS tumor matrix: comparison with amniotic and in vitro networks. *Am. J. Pathol.* 132:278–291.

Yurchenco, P. D., and J. C. Schittny. 1990. Molecular architecture of basement membranes. *FASEB (Fed. Am. Soc. Exp. Biol.) J.* 4:1577–1590.

Yurchenco, P. D., E. C. Tsilibary, A. S. Charonis, and H. Furthmayr. 1985. Laminin polymerization in vitro: evidence for a two-step assembly with domain specificity. *J. Biol. Chem.* 260:7636–7644.

Yurchenco, P. D., Y.-S. Cheng, and J. C. Schittny. 1990. Heparin modulation of laminin polymerization. *J. Biol. Chem.* 265:3981–3991.